The opening of the two pores of the Hv1 voltage-gated proton channel is tuned by cooperativity

Francesco Tombola[1,2], **Maximilian H. Ulbrich**[2], **Susy C. Kohout**[2], and **Ehud Y. Isacoff**[2,3,*]

[1] Department of Physiology and Biophysics, University of California, Irvine, CA 92697

[2] Department of Molecular and Cell Biology, University of California, Berkeley, CA 94720

[3] Material Science Division and Physical Bioscience Division, Lawrence Berkeley National Laboratory, Berkeley, CA 94720

SUMMARY

In voltage-gated sodium, potassium, and calcium channels the functions of ion conduction and voltage sensing are performed by two distinct structural units: the pore domain and the voltage-sensing domain (VSD). In the Hv1 voltage-gated proton channel, the VSD has the remarkable property of performing both functions. Hv1 was recently found to dimerize and to form channels made of two pores. However, the channels were also found to function when dimerization was prevented, raising a question about the functional role of dimerization. Here we show that the two subunits of the Hv1 dimer influence one another during gating, with positive cooperativity shaping the response to voltage of the two pores. We also find that the two voltage sensors undergo conformational changes that precede pore opening and that these conformational changes are allosterically coupled between the two subunits. Our results point to a major role of dimerization in the modulation of Hv1 activity.

Keywords

voltage sensor; proton current; allosteric interactions; gating modifier; total internal reflection microscopy; voltage-clamp fluorometry

INTRODUCTION

Voltage-gated proton channels are expressed in a large variety of excitable and non-excitable cells, where they serve different functions, such as acid extrusion from neurons, muscles, and epithelial cells,[1] and regulation of reactive oxygen species production by the NADPH oxidase in phagocytic cells [2–4]. Hv1, the first -and so far only- member of the voltage-gated proton channel family to be cloned,[5, 6] contains the typical four transmembrane segments of a voltage-sensing domain (VSD), but lacks the two transmembrane segments that form the pore domain in other voltage-gated channels (Fig.

[*]To whom correspondence should be addressed: ehud@berkeley.edu.

1a).[5], [6] The Hv1 protein was recently found to form dimers in which each VSD subunit has its own proton pore and gate, and the cytosolic C-terminus of the channel was shown to be responsible for dimerization.[7–9] Unlike most other channels made of multiple subunits, Hv1 was found to function also when dimerization was prevented by C-terminus substitution[7] or cleavage.[8] This posed an interesting problem. If the two subunits of Hv1 can work separately, why do they form dimers? Do they gain any new functional feature by dimerization?

In tetrameric voltage-gated channels four VSDs control a single pore domain. These VSDs can interact with each other indirectly through their individual coupling to the pore domain [10]. Upon depolarization, a series of independent transitions brings the individual subunits to an activated state. When all four subunits are in this state the channel can undergo a final conformational transition that involves the opening of the gate in the pore domain and is highly cooperative between the four VSDs.[11] This final cooperative transition is crucial in shaping the voltage dependence of channel activation.[12–16]

We explored the possibility that subunit interaction sculpts function in the human Hv1 channel, employing two complementary approaches that were used earlier in the study of gating in the tetrameric voltage-gated channels, first by studying the gating of the subunits with different voltage dependencies within a dimer, and second, using voltage clamp fluorometry (VCF) to monitor the structural rearrangements of one subunit in order to ask whether it is influenced by mutations in the neighboring subunit.

We find that the opening of one Hv1 subunit substantially increases the probability for the other subunit to open. As a result, the two pores in the dimer tend to be in the same state, either both closed or both open. We provide evidence for the involvement of a conserved charged residue in the VSD, which plays a direct role in voltage sensing in other voltage-gated channels, in the allosteric coupling between Hv1 subunits. We use VCF to track the movements of the voltage sensor of an Hv1 subunit labeled with an environment-sensitive fluorophore. We find that the sensor movement is strongly altered by co-expression of a non-labelable subunit that has distinct gating properties, providing support for cooperativity. Our observations indicate that there is a substantial difference in the way the sensors are coupled in Hv1 compared to other voltage-gated channels.

RESULTS

Co-expression of 153C and WT subunits suggests cooperative gating

To investigate whether the two subunits in the Hv1 channel are functionally coupled, we needed ways to distinguish the two subunits in the dimer. We performed a mutagenesis scan on the Hv1 protein to find mutations that alter its voltage sensitivity. The Hv1 mutants were expressed in *Xenopus* oocytes and their proton currents were measured from inside-out membrane patches. We identified mutant E153C in which the voltage dependence of opening (G-V) is negatively shifted by more than 50 mV compared to wild type (WT) (Fig. 1 and Table 1). We then studied the behavior of channels formed by co-expression of 153C and WT subunits. We wanted to make sure to express the 153C subunit at the same level as the WT subunit. To determine expression levels, we tested different amounts of injected

RNA, and determined channel density by single molecule counting of mEGFP-tagged channels in total internal reflection fluorescence (TIRF) microscopy.[17] The RNA levels were adjusted to yield equal density of fluorescent spots when expressing WT-mEGFP alone, 153C-mEGPF alone, or when expressing unlabelled WT and 153C-mGFP together (Fig. 1c). Using the RNA ratio that ensures equal expression of WT and 153C subunits, we examined the G-V of Hv1 channels produced by their co-expression. The G-V of WT + 153C was much more similar to the G-V of channels made of two WT subunits than to the G-V of channels made of two 153C subunits (Fig. 1 and Table 1). This result suggests that the WT subunit exerts a strong influence on the 153C subunit, i.e. that there is cooperativity in gating of Hv1 channels.

153C-WT and WT-153C linked dimers confirms cooperative gating

To perform a quantitative study of cooperativity a precise control of subunit stoichiometry was required. To specify dimer composition on the plasma membrane we produced Hv1 constructs in which two subunits are linked together by a flexible 17-amino-acid-long linker. [7] The 153C mutant was positioned either as the first subunit (153C-WT) or second subunit (WT-153C) and the behavior of these linked heterodimers was compared to the linked 153C-153C and WT-WT homodimers (Fig. 2a). We found that the linkage of the subunits did not affect the behavior of the channels, since we observed the same shift in G-V between 153C-153C and WT-WT linked dimers that we observed between unlinked 153C and WT homodimers (Fig. 2b and Table 1).

We reasoned that if the opening of one subunit in the Hv1 dimer *does not* alter the likelihood of opening of the other subunit (i.e. if gating is independent), then the WT subunit should open with the same voltage dependence regardless of whether it is dimerized with another WT subunit or with a 153C subunit, and the same thing should happen to the 153C subunit. This would mean that the G-V curve for the heterodimers should be a linear combination of the G-V curves for the two homodimers, weighted for the relative contribution to the total proton current of each open subunit (black line in Fig. 2c). To determine the weights of these contributions, the 153C and WT subunits were individually compared to a common reference subunit of known contribution. As explained in the Supplementary Methods (Supplementary Fig. 1), we found that in the 153C-WT and WT-153C dimers the 153C subunit contributes 43% to the total current, with the WT subunit contributing 57%.

A deviation of the G-Vs for the heterodimers from the sum of G-Vs for the homodimers would indicate that the opening of one subunit changes the probability of opening of the other subunit, i.e. that gating is cooperative. We found that the G-Vs of the heterodimers differ from the sum of the G-Vs of the homodimers (Fig. 2c). The difference is particularly evident at the foot of the G-Vs (arrowhead in Fig. 2c). This result indicates that the two subunits of Hv1 do influence each other during gating.

Cooperativity confirmed with distinct gating mutant

Having studied the 153C mutant that shifts the voltage dependence of gating in the negative direction, we searched for other manipulations that would shift the voltage dependence in the opposite direction. Extracellular Zn^{2+} is known to affect the gating of voltage-gated

proton channels.[18] In the presence of Zn^{2+}, stronger depolarizations are required to open the channels (G-V is shifted to more positive potentials). We found the effect of Zn^{2+} to be internal to the single subunit. For this determination we compared the effect of Zn^{2+} on Hv1 WT to Hv1 that was monomerized. Monomerization was achieved by replacing the cytoplasmic dimerization domain of Hv1 with the N and C-termini of the *Ciona intestinalis* Voltage Sensitive Phosphatase (Ci-VSP).[19] The resulting N_{VSP}-Hv1-C_{VSP} chimera[7, 20] was previously shown to be monomeric, like Ci-VSP.[20] We found that Zn^{2+} inhibition at about the midpoint of the G-V was preserved in the chimera (Supplementary Figure 2).

Two histidine residues (H140 and H193) were previously reported to play a key role in Zn^{2+} binding to Hv1 (ref. [5]) The double mutant Hv1 H140A H193A was shown to be insensitive to concentrations of Zn^{2+} up to 100 μM, whereas the IC_{50} for Zn^{2+} of the WT channel was approximately 2 μM.[5] We used extracellular Zn^{2+}, together with the mutation I218S, to shift the G-V of the channel to highly positive potentials (Supplementary Fig. 3).

We constructed an Hv1 subunit with the mutations H140A H193A, to eliminate Zn^{2+} sensitivity (Supplementary Fig. 3), and with the additional mutation N214C which allows us to selectively block the pore of the subunit with the thiol-modifying agent [2-(Trimethylammonium)ethyl]-methanethiosulfonate (MTSET) added intracellularly.[7]

Following a strategy similar to that used for the 153C and WT subunits, we asked whether the H140A H193A N214C, MTSET-sensitive (MS) subunit and the 218S Zn^{2+} sensitive (ZS) subunit influence each other during gating, when they are co-assembled into heterodimers. We, again, looked for deviation of the heterodimer G-V from the sum of the G-Vs of the homodimers. Because the MS subunit can be selectively blocked by MTSET we did not need to determine the relative numbers of the two subunits on the plasma membrane using TIRF microscopy as we did for the non-linked 153C and WT subunits. We determined instead how much co-expressed MS and ZS subunits contribute to the total proton current from the percentage of current inhibition produced by MTSET (Fig. 3a).

We recorded G-Vs from patches excised from oocytes co-expressing MS and ZS subunits in the presence of 25 μM Zn^{2+} in the pipette solution. At the end of each recording, MTSET (1 mM final concentration) was added to the intracellular solution (bath) to block the current flowing through the MS subunit (Fig. 3b, black circles). From the fraction of MTSET-inhibited current (Fig. 3c, black bars) we determined the fraction of MS and ZS subunits in the patch (Fig. 3c gray bars, see methods). We compared the G-V of the channels made by the co-expression of MS and ZS subunits with the G-Vs of MS/MS and ZS/ZS homodimers (Fig. 3d and Table 1). All the measurements were made under the same conditions (Zn^{2+} in the pipette). The results were also compared to the G-V predicted for independent gating of the two subunits (Fig. 3e, continuous line).

The G-V of the channels made of MS and ZS subunits clearly deviates from the G-V predicted for independent gating. This means that the combined effects of mutation 218S and Zn^{2+} binding to the ZS subunit alter the gating of the MS subunit, which does not bind Zn^{2+}. On the other hand, the gating of the ZS subunit is altered by the MS subunit. This

mutual perturbation of gating indicates that the two subunits of Hv1 are allosterically coupled and confirms the results obtained with the 153C and WT subunits.

Quantification of cooperativity

Co-expression of MS and ZS subunits is expected to result mostly in MS/ZS heterodimers and smaller fractions of MS/MS and ZS/ZS homodimers. Both the hetero-and homodimers will contribute to the G-V. It is reasonable to assume that the two different subunits assemble into dimers with equal probabilities,[9] so that the fractions of hetero- and homodimers at the plasma membrane follow a binomial distribution. Because the fractions of MS and ZS subunits on the plasma membrane are known (from the percentage of current inhibition by MTSET), it is possible to calculate the contributions to the G-V of the homodimers. If we subtract these homodimer contributions from the total G-V, what is left is the contribution of the MS/ZS heterodimers (see Methods for details). This MS/ZS heterodimer component of the G-V is reported in Figure 4a (black circles).

We analyzed the MS/ZS heterodimer component of the G-V with the general model for cooperativity originally developed by Koshland, Némethy, and Filmer (KNF model) to describe cooperative ligand binding to enzymes made of multiple allosterically-coupled subunits.[21] For the case of Hv1, namely a dimer made of two interacting pores, the model describes cooperativity as an increase (or decrease) in open probability of one subunit associated with the opening of the other subunit (Fig. 4b and Supplementary Fig. 4). The change in open probability is quantified by the parameter φ. If the open probability of a given subunit is the same, regardless whether or not the other subunit is already open, there is no cooperativity and $\varphi = 1$. Positive cooperativity is characterized by values of φ larger than 1. For example, $\varphi = 10$ means that one subunit is 10 times more likely to open when the other subunit is already open than when it is closed. The opening transitions of each subunit are described as sequential events, and the equilibrium constant K describes the voltage dependence of opening of each subunit. We used the model to calculate the cooperativity factors based on the voltage dependences of the homodimers (labeled as A,A or B,B) and of the heterodimer (labeled as A,B). The system of MS/MS, MS/ZS and ZS/ZS dimers could be described by a single cooperativity factor $\varphi = (\varphi_{MS,MS} = \varphi_{MS,ZS} = \varphi_{ZS,ZS}) = 60 \pm 35$ (Fig. 4a, Supplementary Fig. 5, see Methods). This large φ value indicates robust positive cooperativity between subunits. The observation that the same φ factor could be applied to homo- and heterodimers indicates that the manipulations used to differentiate the voltage dependence of gating of the ZS subunit from that of the MS subunit do not alter the coupling between subunits.

Unlike the situation with the MS/ZS heterodimers, analysis of the 153C-153C, 153C-WT and WT-WT linked dimers with the KNF model failed to recreate the G-V of the heterodimers with a single value for the φ factor (Supplementary Fig. 6, black line). This suggests that the coupling between subunits is perturbed by the 153C mutation. We considered two scenarios that could have this effect: 1) One mutated subunit in the dimer is sufficient to alter coupling ($\varphi_{153C,153C} = \varphi_{153C,WT} \neq \varphi_{WT,WT}$ or $\varphi_{153C,153C} = \varphi_{WT,WT} \neq \varphi_{153C,WT}$), and 2) Coupling is perturbed only when both subunits carry the mutation ($\varphi_{153C,153C} \neq \varphi_{153C,WT} = \varphi_{WT,WT}$). Exploring a range of cooperativity estimated

from the Zn^{2+} experiments on MS/ZS of 60 ± 35 ($25 \quad \varphi \quad 95$) for unperturbed dimers, we find that the G-V of the 153C-WT heterodimer can be best described by Scenario 1 in the case of $\varphi_{153C,153C} = \varphi_{WT,WT} = 95$, $\varphi_{153C,WT} = 23 \pm 2$ (Fig. 4a, see Methods). This analysis is consistent with coupling being partially disrupted (cooperativity reduced) when one subunit has the 153C mutation. In addition, the reduction in cooperativity caused by a mutated subunit is found to depend on whether or not the other subunit is also mutated at the same position ($\varphi_{153C,153C} \quad \varphi_{153C,WT}$). These findings strongly suggest that glutamate 153, in the middle of the S2 segment of Hv1 (Fig. 1a), is involved in the coupling between subunits.

We then wondered what the effect of the E153C mutation would be under conditions in which coupling between subunits is not possible, i.e. in the monomerized version of Hv1, N_{VSP}-Hv1-C_{VSP} [20], described above. The E153C mutation did not cause an appreciable shift in G-V in the chimera (Supplementary Fig. 7). This lack of effect supports the idea that, in the native Hv1 dimer, E153 is involved in the coupling between subunits.

Hv1 gating occurs through multiple VSD transitions

So far we have described pore opening in each of the two Hv1 subunits as a two-state process, from one closed state to one open state. However, the VSDs of other voltage-gated ion channels are known to transition between multiple states before pore opening. We set out to investigate whether the VSDs of Hv1 also visit multiple states during gating. We used voltage clamp fluorometry[22] to detect conformational transitions associated with the gating process. Several positions on the extracellular end of the S4 segment were individually substituted with cysteine. The resulting mutant channels were expressed in oocytes and labeled with the thiol-reactive pH-insensitive fluorophore 2-((5(6)-tetramethylrhodamine)carboxylamino)ethyl-methanethiosulfonate (TAMRA-MTS), which reports on local environment changes produced by conformational transitions. Fluorescence intensity and proton current were recorded simultaneously under two-electrode voltage clamp. Substitution F195C produced the largest fluorescence changes (Fs). As a result, we selected this attachment site mutation for our study. At pH 7.4, we measured fluorescence changes with multiple components (Fig. 5a, gray traces). Upon depolarization a fast increase in fluorescence intensity (fast positive component) was followed by a slow decrease (slow negative component). A positive fluorescence component is produced if the sign of the F matches the sign of the voltage change (F/ V>0). The opposite is true for a negative component (F/ V<0). The presence of the two components indicates that the VSDs of Hv1 undergo at least two distinct conformational changes during gating. The fast fluorescence component precedes channel opening (compare gray current and gray fluorescence traces in Fig. 5a).

Voltage-gated proton channels are known to conduct more current when the intracellular pH is decreased. This is due to two distinct factors: 1) low intracellular pH means higher concentration of the charge carrier flowing through the channels and, 2) the channels are pH-modulated and open more readily at low intracellular pH.[23] We wondered whether in Hv1 the effect of pH on gating is associated with changes in the conformational transitions of the voltage sensor that lead to opening. After recording current and fluorescence changes at pH 7.4, the extracellular medium was exchanged with acetate solution at pH 6.3 (see

Methods) and the measurements on current and fluorescence were repeated (Fig. 5a, black traces). The extracellular acetate buffer produces a cytosolic acidification of the oocyte to pH 6.1.[24] In the presence of acetate, the slow negative component of the fluorescence signal became faster and larger in size, and competed with the early positive component. As a result, the initial positive F was reduced in size. These observations reveal that acidification does accelerate the conformational changes of the voltage sensor leading to opening.

Voltage-sensing transitions are tightly coupled between Hv1 subunits

So far we have shown that the gates in the two subunits of the Hv1 channel are allosterically coupled and work cooperatively; but what about the voltage sensors? Are they also allosterically coupled? In voltage-gated potassium channels, pore opening is achieved by a highly cooperative conformational change in the voltage sensors of the four subunits.[11–15, 25, 26] This conformational change is the last of a series of transitions that occur in each VSD upon membrane depolarization. The early transitions of the voltage sensors in these channels are weakly coupled between subunits and do not contribute significantly to the overall cooperativity of the opening process. We set out to investigate whether this was true also for the voltage sensors of Hv1.

We co-expressed the 195C and 218S Hv1 subunits in oocytes and labeled the channels with TAMRA-MTS. The 218S subunit was present in excess to minimize the fraction of 195C/195C homodimers and favor the assembly of 195C/218S heterodimers and 218S/218S homodimers. Of the 195C/218S and 218S/218S channels, the 218S/218S are "invisible" in terms of the fluorescence recordings because the 218S subunit is not labeled, so that the fluorescence signal in the co-injection experiment will come predominantly from the 195C/218S heterodimer.

We compared the Fs elicited by depolarization in oocytes co-expressing the 195C and 218S subunits with the Fs from oocytes expressing the 195C subunit alone. All the measurements were carried out in an extracellular acetate solution at pH 6.3 to maximize channel activation. At positive voltages, the Fs from the 195C/195C homodimers were characterized by a positive fast component followed by a negative slow component. At negative voltages only the fast fluorescence component was visible (Fig. 5b). The Fs from the 195C/218S heterodimer only contained the negative slow component, while the fast component was missing at all voltages (Fig. 5c). An examination of the fluorescence-voltage relationships (F-Vs) shows that the difference in total F between homo- and heterodimers is maximal at negative voltages due to the lack of the fast component in the heterodimer (Fig. 5d).

Thus, dimerization with the 218S subunit changes the way the voltage sensor moves in the 195C subunit. Early conformational transitions that precede pore opening in the 195C subunit turn out to be the most affected by the 218S subunit, suggesting that they are coupled. This finding, combined with the observed effect of one subunit on the G-V of its dimeric partner, suggests that the coupling between subunits in Hv1 involves both voltage-sensing and opening transitions, and so it differs substantially from the coupling between Kv channel subunits.

DISCUSSION

The Hv1 protein forms dimers in which each VSD subunit has its own proton pore and gate. [7–9] Unlike most other channels made of multiple subunits, Hv1 functions when it is "monomerized".[7, 8] Our experiments show that although each VSD is a separable entity, their association in the dimer enables them to gate cooperatively. The cooperativity is substantial and positive, with the opening of one Hv1 subunit increasing the probability of opening of the other subunit by ~60-fold. This means that the two pores of Hv1 tend to be in the same state, either both closed or both open (Fig. 6).

The total charge that needs to be moved across the membrane electric field in order to open a voltage-gated sodium or potassium channel (gating charge) is 12-13.5e_o [27–31]. This amounts to a gating charge of 3–3.4e_o for each VSD, with the 4 VSDs cooperatively gating one pore. Four arginine residues in the VSD S4 segment are known to give the major contribution to the charge [30, 31]. The total gating charge of voltage-gated proton channels has been estimated to be ~6e_o [1]. This led to a conundrum when it was discovered that Hv1 has two pores, each controlled by one VSD, since it implied that each VSD would have a gating charge of ~6e_o, even though S4 alignments showed that Hv1 is actually missing the fourth arginine (R4).[5–7] Our discovery that the two VSDs of the Hv1 dimer gate cooperatively provides an answer to this problem, suggesting that each VSD of Hv1 has a gating charge of ~3e_o.

The opening kinetics of Hv1 channels is sigmoidal. This sigmoidicity, also observed in native voltage-gated proton channels, led to an earlier proposal that activation proceeds in more than one step.[1] It has not been possible to measure gating currents from proton channels, leaving it unclear until now whether there are any steps of voltage sensing that precede opening. Using voltage-clamp fluorometry to track the movement of the voltage-sensing S4 in real time during gating, we find that there is, indeed, at least one voltage-sensing transition that precedes pore opening in Hv1.

We used VCF as an independent way of testing for cooperativity in gating, as done earlier in the Shaker K^{+} channel.[15, 26] Our experiments show that the readout of S4 motion is altered when an Hv1 subunit, with a cysteine added at the outer end of S4 to serve as a fluorophore attachment site, is co-expressed with a gating mutant subunit. This indicates that the gating of the labeled subunit is influenced by the unlabeled subunit, thus confirming that there is cooperativity between VSDs co-assembled into a dimer. Our kinetic and steady-state analyses indicate that the transition that is most obviously affected by the presence of the mutated subunit is an early phase of voltage sensing. In contrast, in tetrameric voltage-gated K^{+} channels, the early voltage sensing transitions are not coupled, but the opening step is, involving a highly cooperative motion of S4.[14, 15] The difference likely arises from the structural organization of Hv1, in which the VSDs interact directly, as opposed to other voltage-gated channels, in which the VSDs indirectly interact via the pore domain.

We find that the allosteric coupling between Hv1 subunits is influenced by a conserved negatively charged residue, E153, located in the S2 helix. The Shaker homologue of E153, E293, interacts electrostatically with S4 arginines.[32] In the dimeric Hv1, we find that E153C

causes a large shift in the voltage dependence of gating, while there is no such shift in the monomeric version of Hv1. The shift is also strongly reduced in the 153C/WT heterodimer. Our quantification of cooperativity indicates that residue 153 plays an important role in coupling. An involvement of E153 in both voltage-sensing and coupling is consistent with the VCF finding that the VSDs in the Hv1 dimer are coupled during voltage sensing.

Finally, voltage-gated proton currents with distinct properties have been observed in different cell types.[33] For instance, proton currents with an activation time constant of just a few milliseconds are found in snail neurons,[34] while an activation time constant of several seconds is typical of mammalian phagocytes.[1] In principle, the channels carrying these currents could be formed by different gene products or by splice isoforms from one gene. Sequence analysis of the Hv1 gene (HVCN1) predicts three alternative splice isoforms, one of which lacks part of the C-terminus and which might therefore have oligomerization properties different from the full-length isoform studied here. The inter-subunit cooperativity that we observe suggests that dimerization with related gene products could expand the variety of the biophysical properties of the channels and contribute to the observed diversity seen in native proton channels in different cell types.

METHODS

DNA constructs and expression in *Xenopus* oocytes

We made all DNA constructs using the human version of Hv1 (ref. [5]) in the pGEMHE vector, as previously described.[7] For electrophysiological measurements, 50 nl of RNA 0.25-1.5 $\mu g \mu l^{-1}$ were injected into *Xenopus laevis* oocytes. For the determination of the surface-density of mEGFP-tagged channels, RNA concentration was 0.02 $\mu g \mu l^{-1}$ for WT Hv1 (with or without a fused EGFP) and 0.1 $\mu g \mu l^{-1}$ for Hv1 153C fused to EGFP. We maintained the injected cells in medium ND96 as previously described,[7] and allowed protein expression for 1–3 days at 18°C.

Single-molecule TIRF imaging

After treating oocytes expressing mEGFP-labeled Hv1 channels with neuraminidase and hyaluronidase,[35] we manually removed their vitelline membrane, and placed them on high refractive index coverslips (n=1.78, PlanOptik) for fluorescence measurements through an Olympus 100x objective (N.A. 1.65). We used a 488-nm Ar laser for excitation and recoded emission through a 525/50 band-pass filter (Chroma Tech.) with an EMCCD camera (Andor Ixon DV-897 BV). Images were acquired and analyzed as previously described.[17]

Patch-clamp measurements

We performed the measurements in excised inside-out configuration 1-3 days after injection.[36] The bath and pipette solution contained 100 mM 2-(N-morpholino) ethanesulphonic acid (MES), 30 mM tetraethylammonium (TEA) methanesulfonate, 5 mM TEA chloride, 5 mM ethyleneglycol-bis(2-aminoethyl)-N,N,N',N'-tetra-acetic acid (EGTA), adjusted to pH 6.0 with TEA hydroxide. For measurements carried out in the presence of extracellular Zn^{2+}, the pipette solution contained 100 mM MES, 40 mM TEA methanesulfonate, 5 mM TEA chloride, 25 μM $ZnCl_2$, pH 6.0. Cysteine modification with MTSET (Toronto Research

Chemicals) was performed as previously reported.[7] Pipettes had 2.8-4.0 MΩ access resistance. The temperature was 22 ± 2 °C. Current traces were filtered at 1 kHz, sampled at 5 kHz, and analyzed with Clampfit10.2 (Molecular Devices) and Origin7.5 (OriginLab). G-V plots were obtained from tail currents using voltage protocols similar to those described in [7] and fitted by the Boltzmann equation:

$$G/G^{\mathrm{max}}=1/(1+e^{-\frac{ze_O}{kT}(V-V_{1/2})}) \quad (1)$$

Where e_o is the elementary charge, k is the Boltzmann's constant, T is the absolute temperature. Changes in local proton concentration during channel opening[37] were sufficiently small to not significantly distort the measured G-Vs (Supplementary Fig. 7).

We calculated the G-V expected for the heterodimers 153C-WT and WT-153C, in case of two independent pores (black line in Fig. 2c), combining the Boltzmann fits for the G-Vs of homodimers 153C-153C and WT-WT according to the equation:

$$\frac{G_{153C-W}}{G^{\mathrm{max}}_{153C-W}}=\frac{G_{W-153C}}{G^{\mathrm{max}}_{W-153C}}=f_{153C}\frac{G_{153C-153C}}{G^{\mathrm{max}}_{153C-153C}}+(1-f_{153C})\frac{G_{W-W}}{G^{\mathrm{max}}_{W-W}} \quad (2)$$

Where f_{153C} is the fraction of total current carried by the 153C subunit in the linked heterodimers. If the 153C and WT subunits contributed equally to the total current, f_{153C} would be 0.5. As described in the Supplementary Methods, we determined the actual value of f_{153C} and found it to be 0.43 ± 0.02 (n=5). This indicates that a maximally open 153C subunit carries slightly less current than a maximally open WT subunit.

The G-V expected for channels generated by coexpression of MS and ZS subunits in case of two independent pores (black line in Fig. 3e) was calculated combining the Boltzmann fits for the G-Vs of homodimers MS/MS and ZS/ZS according to the equation:

$$\frac{G_{MS/ZS}}{G^{\mathrm{max}}_{MS/ZS}}=f_{MS}\frac{G_{MS/MS}}{G^{\mathrm{max}}_{MS/MS}}+(1-f_{MS})\frac{G_{ZS/ZS}}{G^{\mathrm{max}}_{ZS/ZS}} \quad (3)$$

Where the f_{MS} is the fraction of total current carried by the MS subunit. We determined the fraction of MS subunits for each recording from the % of current inhibition caused by MTSET treatment (Fig. 3b-c). The average value of f_{MS} turned out to be 0.42 ± 0.04 (n=5), using an RNA ratio of MS and ZS subunits of 3:1.

Voltage-clamp fluorometry

We performed voltage-clamp fluorometry 2-3 days after oocyte injection (50 nl of RNA 1.0-2.0 μg μl^{-1}), as previously described.[22] We blocked native cysteines by treatment with 1 mM glycine maleimide within the first hour post-injection, before newly translated Hv1 channels appeared on the cell surface. Before recording, we incubated the cells with 25 μM TAMRA-MTS (Toronto Research Chemicals) for 30 minutes at 0 °C and then extensively washed in ND96. Recordings were performed in ND96 at pH 7.4, and in acetate solution at

pH 6.3. The acetate solution contained 55mM sodium methanesulfonate, 55mM sodium acetate, 10mM MES, 2 mM MgCl$_2$, adjusted to pH 6.3 with NaOH.

We acquired fluorescence signals through a 20X 0.75 NA fluorescence objective (Nikon) on a Nikon Diaphot inverted microscope and a Hamamatsu HC120-05 photomultiplier tube. Excitation filter, emission filter, and dichroic were HQ535/50, HQ610/75, and Q565LP respectively (Chroma Tech.). A Dagan CA-1 amplifier (Dagan Corporation) was used for two-electrode voltage clamp. The signal from the photomultiplier was low-pass filtered at 2 kHz and sampled at 10 kHz through a Digidata-1440A controlled by pClamp10 (Molecular Devices). We normalized F-Vs between minimum and maximum fluorescence levels.

Gating model for the two pores of Hv1

We adapted the general Koshland-Némethy-Filmer (KNF) model of subunit cooperativity[21] to describe the cooperative opening of the two pores of Hv1. The processes related to opening for the homo- and heterodimers are reported in Figure 4b and Supplementary Figure 4. Transitions from close (C) to open (O) state are represented by an equilibrium constant K, which describes the intrinsic voltage sensitivity of each subunit, and a cooperativity parameter φ, which accounts for the global influence of one subunit over its neighbor. These parameters are defined as:

$$K_A=[O_A]/[C_A], \qquad K_B=[O_B]/[C_B]$$
$$\phi_{A,A}=\frac{[O_A O_A]\,[C_A C_A]}{[O_A C_A]\,[C_A O_A]}, \quad \phi_{B,B}=\frac{[O_B O_B]\,[C_B C_B]}{[O_B C_B]\,[C_B O_B]}, \quad \phi_{A,B}=\phi_{B,A}=\frac{[O_A O_B]\,[C_A C_B]}{[O_A C_B]\,[C_A O_B]}$$

Using this model the voltage dependence of heterodimers A,B can be reconstructed from the voltage dependences of homodimers A,A and B,B according to equation (4):

$$\frac{G_{A,B}}{G_{A,B}^{\max}}$$
$$=\frac{1}{2}\frac{\phi_{A,B}+\phi_{A,A}(e^{x_A}+2\sqrt{Q_A}-1)^{-1}+\phi_{B,B}(e^{x_B}+2\sqrt{Q_B}-1)^{-1}}{\frac{\phi_{A,B}}{2}+\phi_{A,A}(e^{x_A}+2\sqrt{Q_A}-1)^{-1}+\phi_{B,B}(e^{x_B}+2\sqrt{Q_B}-1)^{-1}+2\phi_{A,A}\phi_{B,B}[(e^{x_A}+2\sqrt{Q_A}-1)(e^{x_B}+2\sqrt{Q_B}-1)]^{-1}}$$

where:

$$Q_A=(\phi_{A,A}-1)e^{x_A}+\frac{1}{4}(1+e^{x_A})^2, \quad x_A=\frac{z_{A,A}\,e_o}{kT}(V-V_{1/2(A,A)})$$
$$Q_B=(\phi_{B,B}-1)e^{x_B}+\frac{1}{4}(1+e^{x_B})^2, \quad x_B=\frac{z_{B,B}\,e_o}{kT}(V-V_{1/2(B,B)})$$

The derivation of this equation is reported in the Supplementary Methods.

If the manipulations used to alter subunit voltage sensitivity do not significantly affect coupling, the φ parameter is the same for homo- and heterodimers ($\varphi = \varphi_{A,A} = \varphi_{A,B} = \varphi_{B,B}$). In this case, the G-V for the heterodimers can be fitted by equation (4) with φ as only free parameter. As discussed in the result section, this condition was met by MS/ZS heterodimers but not by 153C-WT heterodimers. In the case of co-expressed MS and ZS subunits, MS/ZS

heterodimers contribute the most to the measured G-V. But the contributions from MS/MS and ZS/ZS homodimers are not negligible, so they need to be subtracted from the total G-V before applying equation (4). If the subunits assemble randomly, the fractions of dimers with different compositions follow a binomial distribution defined by the fraction of MS and ZS subunits. We calculated the distribution and isolated the G-V component contributed by the heterodimers, as explained in the Supplementary Methods. The fittings with equation (4) were performed with Mathematica (Wolfram Res.) using the built-in NonlinearRegress function.

Supplementary Material

Refer to Web version on PubMed Central for supplementary material.

Acknowledgments

References

1. Decoursey TE. Voltage-gated proton channels and other proton transfer pathways. Physiol Rev. 2003; 83:475–579. [PubMed: 12663866]

2. Henderson LM, Chappell JB, Jones OT. The superoxide-generating NADPH oxidase of human neutrophils is electrogenic and associated with an H+ channel. Biochem J. 1987; 246:325–9. [PubMed: 2825632]

3. DeCoursey TE, Morgan D, Cherny VV. The voltage dependence of NADPH oxidase reveals why phagocytes need proton channels. Nature. 2003; 422:531–4. [PubMed: 12673252]

4. Ramsey IS, Ruchti E, Kaczmarek JS, Clapham DE. Hv1 proton channels are required for high-level NADPH oxidase-dependent superoxide production during the phagocyte respiratory burst. Proc Natl Acad Sci U S A. 2009; 106:7642–7. [PubMed: 19372380]

5. Ramsey IS, Moran MM, Chong JA, Clapham DE. A voltage-gated proton-selective channel lacking the pore domain. Nature. 2006; 440:1213–6. [PubMed: 16554753]

6. Sasaki M, Takagi M, Okamura Y. A voltage sensor-domain protein is a voltage-gated proton channel. Science. 2006; 312:589–92. [PubMed: 16556803]

7. Tombola F, Ulbrich MH, Isacoff EY. The voltage-gated proton channel Hv1 has two pores, each controlled by one voltage sensor. Neuron. 2008; 58:546–56. [PubMed: 18498736]

8. Koch HP, et al. Multimeric nature of voltage-gated proton channels. Proc Natl Acad Sci U S A. 2008; 105:9111–6. [PubMed: 18583477]

9. Lee SY, Letts JA, Mackinnon R. Dimeric subunit stoichiometry of the human voltage-dependent proton channel Hv1. Proc Natl Acad Sci U S A. 2008; 105:7692–5. [PubMed: 18509058]

10. Long SB, Campbell EB, Mackinnon R. Crystal structure of a mammalian voltage-dependent Shaker family K+ channel. Science. 2005; 309:897–903. [PubMed: 16002581]

11. Tombola F, Pathak MM, Isacoff EY. How Does Voltage Open an Ion Channel? Annu Rev Cell Dev Biol. 2006; 22:23–52. [PubMed: 16704338]

12. Zagotta WN, Hoshi T, Aldrich RW. Shaker potassium channel gating. III: Evaluation of kinetic models for activation. J Gen Physiol. 1994; 103:321–62. [PubMed: 8189208]

13. Schoppa NE, Sigworth FJ. Activation of Shaker potassium channels. III. An activation gating model for wild-type and V2 mutant channels. J Gen Physiol. 1998; 111:313–42. [PubMed: 9450946]

14. Ledwell JL, Aldrich RW. Mutations in the S4 region isolate the final voltage-dependent cooperative step in potassium channel activation. J Gen Physiol. 1999; 113:389–414. [PubMed: 10051516]

15. Pathak M, Kurtz L, Tombola F, Isacoff E. The cooperative voltage sensor motion that gates a potassium channel. J Gen Physiol. 2005; 125:57–69. [PubMed: 15623895]

16. Yifrach O, MacKinnon R. Energetics of pore opening in a voltage-gated K(+) channel. Cell. 2002; 111:231–9. [PubMed: 12408867]

17. Ulbrich MH, Isacoff EY. Subunit counting in membrane-bound proteins. Nat Methods. 2007; 4:319–21. [PubMed: 17369835]

18. DeCoursey TE, Cherny VV. Pharmacology of voltage-gated proton channels. Curr Pharm Des. 2007; 13:2400–20. [PubMed: 17692009]

19. Murata Y, Iwasaki H, Sasaki M, Inaba K, Okamura Y. Phosphoinositide phosphatase activity coupled to an intrinsic voltage sensor. Nature. 2005; 435:1239–43. [PubMed: 15902207]

20. Kohout SC, Ulbrich MH, Bell SC, Isacoff EY. Subunit organization and functional transitions in Ci-VSP. Nat Struct Mol Biol. 2008; 15:106–8. [PubMed: 18084307]

21. Koshland DE Jr, Nemethy G, Filmer D. Comparison of experimental binding data and theoretical models in proteins containing subunits. Biochemistry. 1966; 5:365–85. [PubMed: 5938952]

22. Mannuzzu LM, Moronne MM, Isacoff EY. Direct physical measure of conformational rearrangement underlying potassium channel gating. Science. 1996; 271:213–6. [PubMed: 8539623]

23. Cherny VV, Markin VS, DeCoursey TE. The voltage-activated hydrogen ion conductance in rat alveolar epithelial cells is determined by the pH gradient. J Gen Physiol. 1995; 105:861–96. [PubMed: 7561747]

24. Choe H, Zhou H, Palmer LG, Sackin H. A conserved cytoplasmic region of ROMK modulates pH sensitivity, conductance, and gating. Am J Physiol. 1997; 273:F516–29. [PubMed: 9362329]

25. Gagnon DG, Bezanilla F. A single charged voltage sensor is capable of gating the Shaker K+ channel. J Gen Physiol. 2009; 133:467–83. [PubMed: 19398775]

26. Mannuzzu LM, Isacoff EY. Independence and cooperativity in rearrangements of a potassium channel voltage sensor revealed by single subunit fluorescence. J Gen Physiol. 2000; 115:257–68. [PubMed: 10694254]

27. Schoppa NE, McCormack K, Tanouye MA, Sigworth FJ. The size of gating charge in wild-type and mutant Shaker potassium channels. Science. 1992; 255:1712–5. [PubMed: 1553560]

28. Noceti F, et al. Effective gating charges per channel in voltage-dependent K+ and Ca2+ channels. J Gen Physiol. 1996; 108:143–55. [PubMed: 8882860]

29. Hirschberg B, Rovner A, Lieberman M, Patlak J. Transfer of twelve charges is needed to open skeletal muscle Na+ channels. J Gen Physiol. 1995; 106:1053–68. [PubMed: 8786350]

30. Aggarwal SK, MacKinnon R. Contribution of the S4 segment to gating charge in the Shaker K+ channel. Neuron. 1996; 16:1169–77. [PubMed: 8663993]

31. Seoh SA, Sigg D, Papazian DM, Bezanilla F. Voltage-sensing residues in the S2 and S4 segments of the Shaker K+ channel. Neuron. 1996; 16:1159–67. [PubMed: 8663992]

32. Papazian DM, et al. Electrostatic interactions of S4 voltage sensor in Shaker K+ channel. Neuron. 1995; 14:1293–301. [PubMed: 7605638]

33. Morgan D, DeCoursey TE. Diversity of voltage gated proton channels. Front Biosci. 2003; 8:s1266–79. [PubMed: 12957841]

34. Thomas RC, Meech RW. Hydrogen ion currents and intracellular pH in depolarized voltage-clamped snail neurones. Nature. 1982; 299:826–8. [PubMed: 7133121]

35. Sonnleitner A, Mannuzzu LM, Terakawa S, Isacoff EY. Structural rearrangements in single ion channels detected optically in living cells. Proc Natl Acad Sci U S A. 2002; 99:12759–64. [PubMed: 12228726]

36. Larsson HP, Baker OS, Dhillon DS, Isacoff EY. Transmembrane movement of the shaker K+ channel S4. Neuron. 1996; 16:387–97. [PubMed: 8789953]

37. Musset B, et al. Detailed comparison of expressed and native voltage-gated proton channel currents. J Physiol. 2008; 586:2477–86. [PubMed: 18356202]
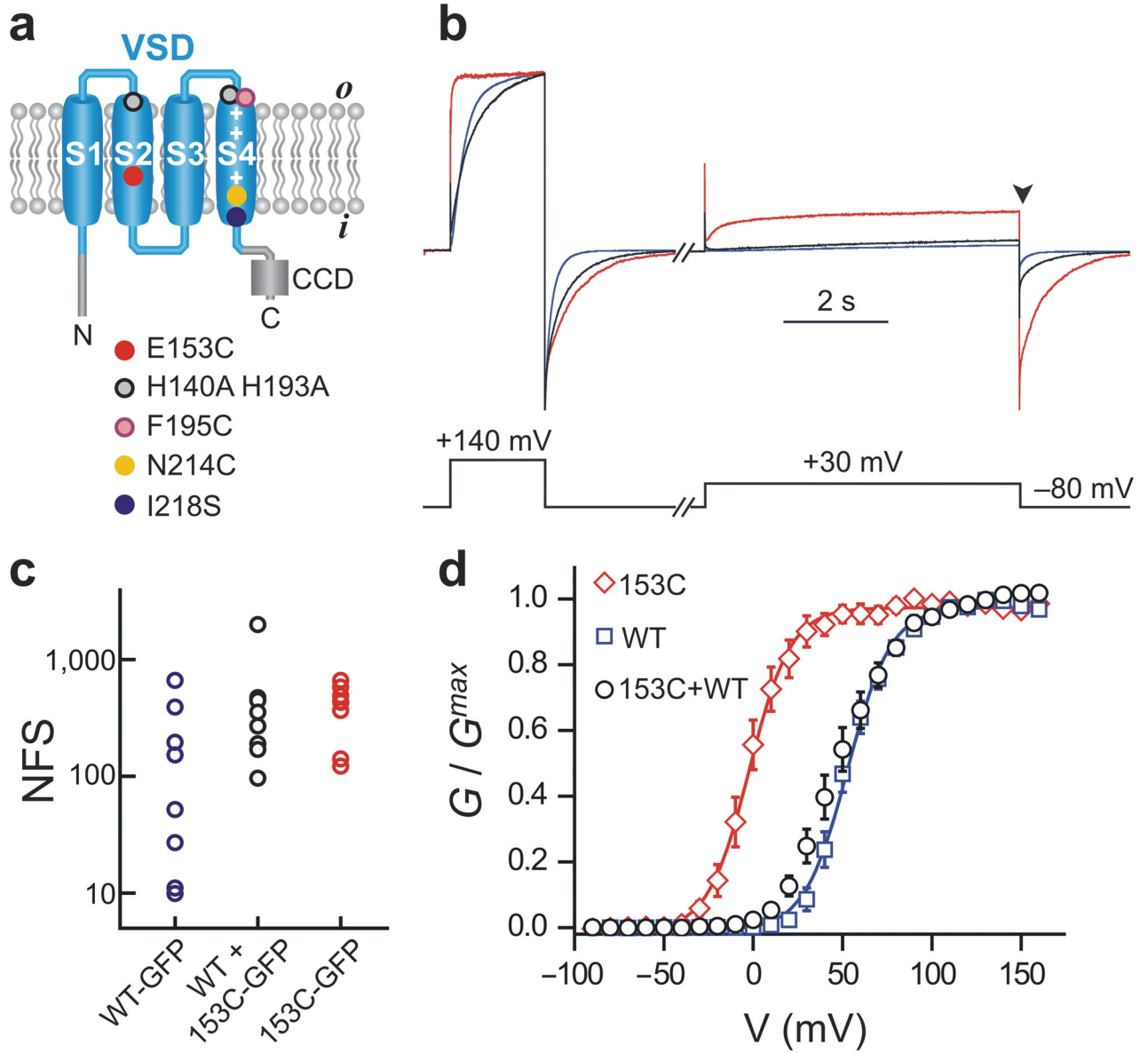
Figure 1.

Gating perturbation of one Hv1 subunit spreads to the neighboring subunits. (**a**) Topologic organization of Hv1 and amino acid substitutions used for altering channel sensitivity to voltage (E153C, I218S), Zn^{2+} (H140A, H193A) or MTSET (N214C), or for labeling the voltage sensor with the environment-sensitive fluorescent dye (F195C). CCD: coiled-coil domain. (**b**) Example of current traces recorded from membrane patches of three different oocytes expressing Hv1 153C (red), Hv1 WT (blue), or co-expressing Hv1 153C with WT (black). $pH_i = pH_o = 6.0$. Traces were normalized to `the maximum value reached at the end of the first depolarization step (+140 mV). cRNAs coding for the WT and 153C subunits were co-injected in a 1:5 ratio to obtain comparable subunit density at the plasma membrane, as determined in **c**. (**c**) Comparison of subunit densities at the cell surface determined by single-molecule counting. Each point represents the total number of

fluorescent spots (NSF) in the field of view ($13\times13~\mu m^2$) from an individual oocyte, counted under total internal reflection fluorescence (TIRF) microscopy. The amount of 153C-GFP RNA injected was 5-fold higher than the amount of WT-GFP RNA. In the co-injection, the WT subunit was not labeled, but the 153C-GFP was (RNA ratio WT:153C = 1:5). (**d**) Voltage dependence of proton conductance of the indicated Hv1 channels. RNA ratio and pH as in **b**. Each point is the average of 4–6 measurements ± s.e.m. Curves are Boltzmann fits. See Table 1 for parameters.
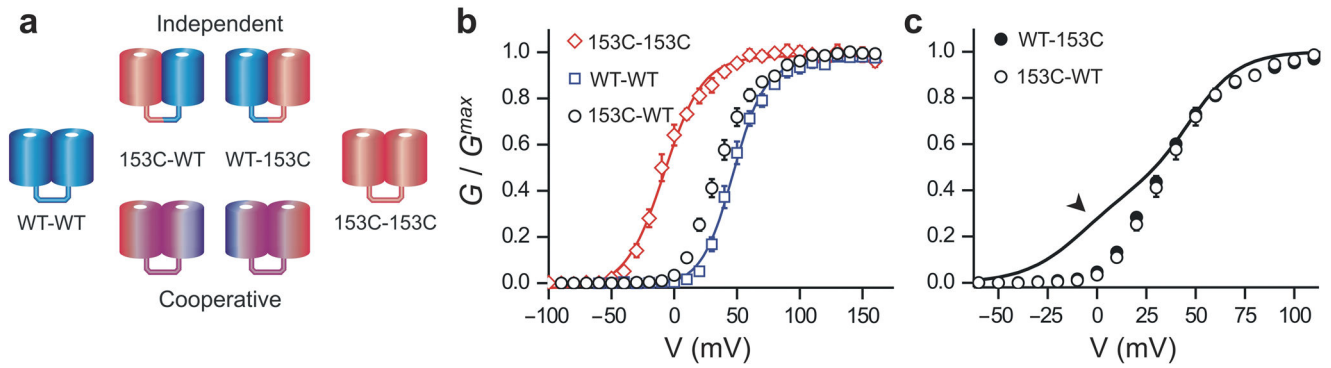
Figure 2.
Cooperative gating in Hv1 linked dimers made of 153C and WT subunits. (**a**) Cartoon representing the possible scenarios for subunit cooperativity in Hv1 linked dimers. Subunits with different colors have different activation properties. Purple shading indicates an influence of one subunit on the other. (**b**) Voltage dependence of proton conductances of the linked 153C–153C and WT-WT homodimers, compared to the voltage dependence of linked 153C-WT heterodimers. See Table 1 for Boltzmann fits. (**c**) Comparison between voltage dependence of the linked 153C-WT and WT-153C heterodimers and the prediction for the independent opening of the two pores (continuous line). $pH_i = pH_o = 6.0$. Error bars are s.e.m., n = 4–6.
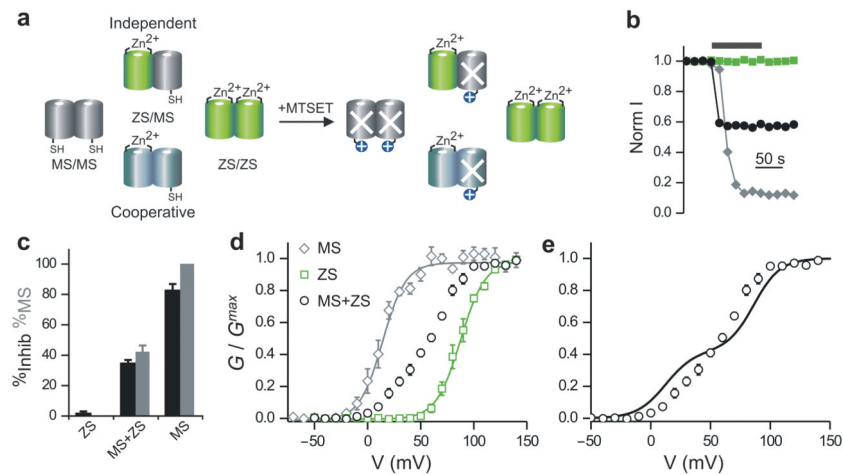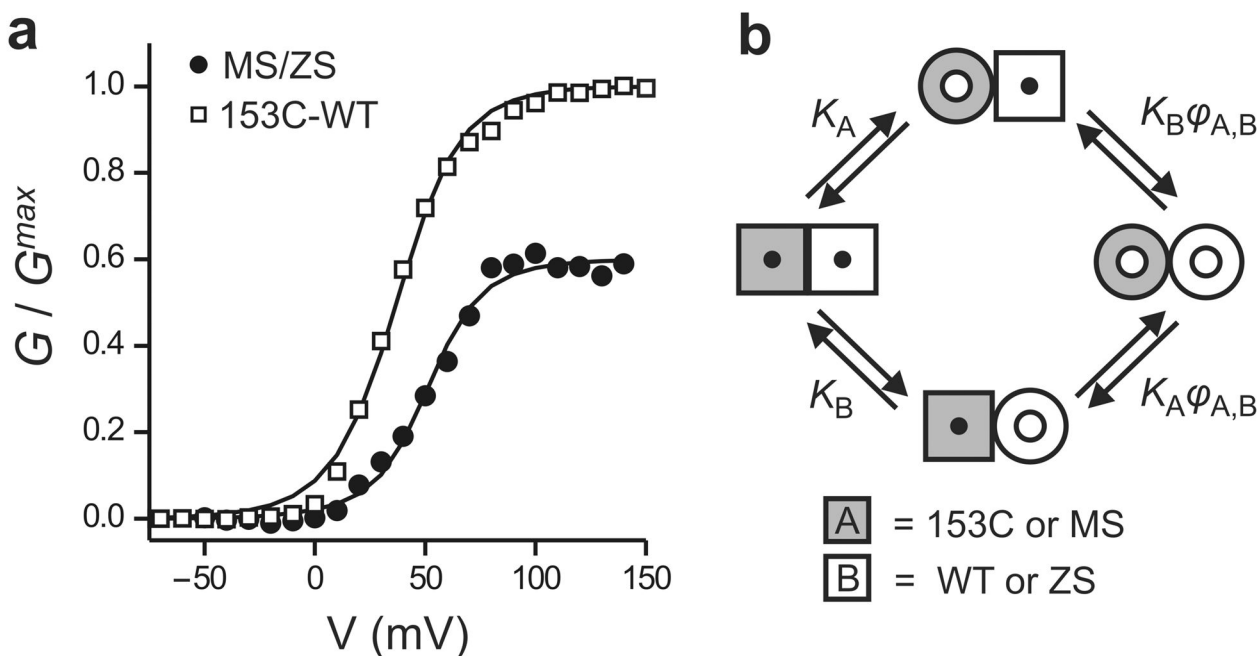
Figure 3.

Cooperative gating in Hv1 dimers made of MS and ZS subunits. (**a**) Assembly of MTSET-sensitive (MS) and Zinc-sensitive (ZS) subunits in homo-and heterodimers. White X indicates blocked MS subunit after MTSET treatment. (**b**) Example of changes in normalized proton currents from membrane patches of oocytes expressing Hv1 MS (gray diamonds), Hv1 ZS (green squares), or co-expressing Hv1 MS with ZS (black circles). 25 μM Zn^{2+} was maintained in the extracellular solution throughout the recordings. $pH_i = pH_o$ = 6.0. Black bar indicates duration of exposure to 1 mM intracellular MTSET. The RNA ratio for the co-expression of MS and ZS subunits was 3:1. (**c**) Quantification of inhibition produced by MTSET for the indicated conditions (black bars). From the extent of proton current inhibition the percentage of MS subunits was calculated (gray bars), as explained in the text. (**d**) Voltage dependence of proton conductance of Hv1 MS and Hv1 ZS, compared to the voltage dependence of the co-injection of Hv1 MS + Hv1 ZS. See Table 1 for Boltzmann fits. Each point is the average of 4–6 measurements ± s.e.m. Recording conditions and RNA ratio were the same as for panels **b** and **c**. (**e**) Comparison between voltage dependence of proton channels produced by co-expression of MS and ZS subunits (open circles), and voltage dependence expected in case of independent opening of the two pores (continuous line, see text).

Figure 4.
Quantification of cooperativity in Hv1. (**a**) Voltage dependence of activation of the MS/ZS heterodimer and the 153C-WT linked dimer fitted with the opening model shown in **b**. For MS/ZS Hv1: $\varphi_{MS,MS} = \varphi_{MS,ZS} = \varphi_{ZS,ZS} = 60 \pm 35$, for153C-WT Hv1: $\varphi_{153C,153C} = \varphi_{WT,WT} = 95$, $\varphi_{153C,WT} = 23 \pm 2$. See text for details. (**b**) Model of opening of the two pores of Hv1. Cooperativity is quantified by the parameter φ, which is the ratio between the open probability of a given subunit when the neighboring subunit is in the open conformation and the open probability of the same subunit when the neighboring subunit is in the closed conformation. $\varphi > 1$ means that the opening of one pore makes it easier for the other pore to open (positive cooperativity). The scheme represents the case of a heterodimer made of subunit A (gray) and subunit B (white) with different voltage dependencies of activation (K_A and K_B). Subunit A can be 153C or MS, and subunit B can be WT or ZS. The transition from square shape to round shape represents the conformational change associated with opening (see also Supplementary Fig.4).
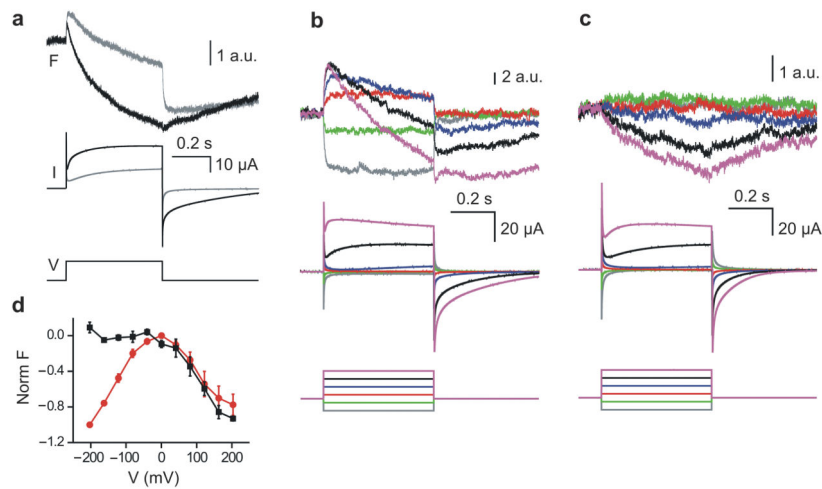
Figure 5.

Hv1 voltage-sensor coupling detected by voltage-clamp fluorometry. (**a**) Voltage sensor movement detected on Hv1 195C labeled with TAMRA-MTS. Changes in fluorescence (F) and proton current (I) were produced by the indicated voltage step (V) from −80 mV to +160 mV. Traces in gray were recorded at pH_o 7.4. Traces in black were recorded from the same oocyte in acetate buffer at pH_o 6.3, which also acidifies the internal solution (see text). (**b–c**) Comparison between voltage sensor movement in labeled 195C/195C homodimers and 195C/218S heterodimers. Heterodimers were produced by co-expressing the Hv1 195C subunit with an excess of the 218S subunit. Fluorescence changes and proton currents were elicited by voltage steps from −200 to +200 mV in 80 mV increments. Holding potential was −80 mV, pH_o was 6.3. (**d**) Normalized F-Vs from labeled oocytes expressing the Hv1 195C subunit (red circles) or co-expressing the 195C and 218S subunits (black squares). Fluorescence was measured at the end of the 500-ms long test-pulse (voltage protocol and recording conditions as in **b–c**. Each point is the average of 5 measurements ± s.e.m.
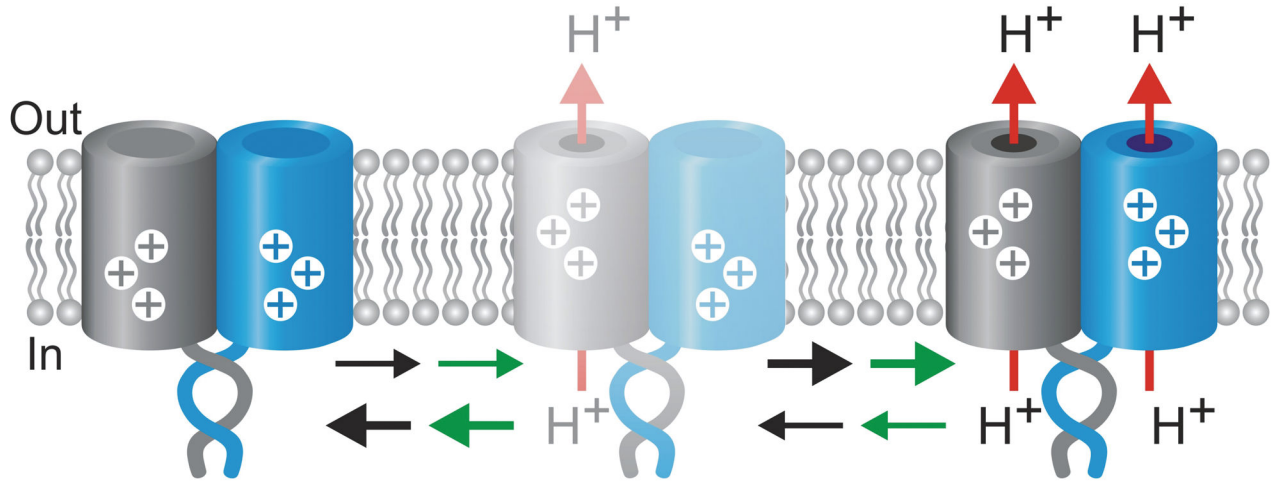
Figure 6.
Proposed basic gating mechanism for the Hv1 channel. Opening of one subunit favors the opening of the neighboring subunit. As a result, the two subunits tend to be in the same state, either both closed or both open. With a cooperativity factor $\varphi = 60$ the total fraction of channels with only one open pore can never be higher than 12%. The represented states are connected by at least two transitions: a voltage sensing transition (black arrows) responsible for the fast component of sensor movement detected by VCF, and an opening transition (green arrows). Based on the similarity between the VSD of Hv1 and the VSDs of other voltage-gated channels, the voltage-sensing process is represented as upward movement of charges (shown in white). The C-termini of the two subunits are shown as coiled-coil.

Table 1

Mean Boltzmann fit parameters (± s.e.m.) for the G-V curves of different Hv1 homodimers (Figs. 1d, 2b, and 3d).

#	Channel	$V_{1/2}$ (mV)	kT/ze$_o$ (mV)	n
1	Hv1 WT	53 ± 3	11.6 ± 0.6	5
2	Hv1 153C	−1.6 ± 3.6	11.4 ± 1.3	4
3	TD WT-WT	47 ± 2	12.6 ± 0.6	4
4	TD 153C-153C	−8.0 ± 1.2	14.9 ± 1.2	5
5	MS/MS + 25 µM Zn^{2+}	13 ± 3	11.4 ± 2.0	5
6	ZS/ZS + 25 µM Zn^{2+}	86 ± 3	11.0 ± 1.0	4

n = number of oocytes; MS = Hv1 H140A-H193A-N214C; ZS = Hv1 I218S.